

See discussions, stats, and author profiles for this publication at: <https://www.researchgate.net/publication/51474171>

# Third-Order Nonlinear Optical Properties of Open-Shell Supramolecular Systems Composed of Acetylene Linked Phenalenyl Radicals

ARTICLE *in* THE JOURNAL OF PHYSICAL CHEMISTRY A · AUGUST 2011

Impact Factor: 2.69 · DOI: 10.1021/jp205259p · Source: PubMed

CITATIONS

22

READS

23

8 AUTHORS, INCLUDING:



Masayoshi Nakano

Osaka University

334 PUBLICATIONS 4,714 CITATIONS

SEE PROFILE



Ryohei Kishi

Osaka University

110 PUBLICATIONS 1,930 CITATIONS

SEE PROFILE



Yasuteru Shigeta

University of Tsukuba

174 PUBLICATIONS 1,804 CITATIONS

SEE PROFILE



Benoît Champagne

University of Namur

400 PUBLICATIONS 8,600 CITATIONS

SEE PROFILE

# Third-Order Nonlinear Optical Properties of Open-Shell Supermolecular Systems Composed of Acetylene Linked Phenalenyl Radicals

Masayoshi Nakano,\* Ryohei Kishi, Kyohei Yoneda, Yudai Inoue, Tomoya Inui, and Yasuteru Shigeta

Department of Materials Engineering Science, Graduate School of Engineering Science, Osaka University, Toyonaka, Osaka 560-8531, Japan

Takashi Kubo

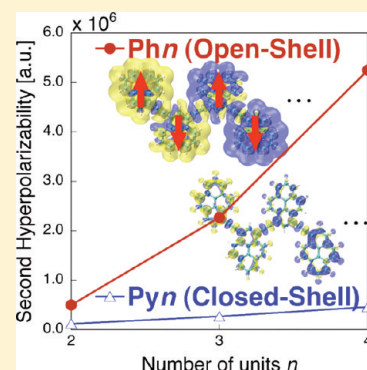
Department of Chemistry, Graduate School of Science, Osaka University, Toyonaka, Osaka 560-0043, Japan

Benoît Champagne

Laboratoire de Chimie Théorique (LCT), Facultés Universitaires Notre-Dame de la Paix (FUNDP), Rue de Bruxelles, 61, B-5000 Namur, Belgium

**S** Supporting Information

**ABSTRACT:** The third-order nonlinear optical (NLO) properties, at the molecular level, the static second hyperpolarizabilities,  $\gamma$ , of supermolecular systems composed of phenalenyl and pyrene rings linked by acetylene units are investigated by employing the long-range corrected spin-unrestricted density functional theory, LC-UBLYP, method. The phenalenyl based superethylene, superallyl, and superbutadiene in their lowest spin states have intermediate diradical characters and exhibit larger  $\gamma$  values than the closed-shell pyrene based superpolyene systems. The introduction of a positive charge into the phenalenyl based superallyl radical changes the sign of  $\gamma$  and enhances its amplitude by a factor of 35. Although such sign inversion is also observed in the allyl radical and cation systems in their ground state equilibrium geometries, the relative amplitude of  $\gamma$  is much different, that is,  $|\gamma(\text{regular allyl cation})/\gamma(\text{regular allyl radical})| = 0.61$  versus  $|\gamma(\text{phenalenyl based superallyl cation})/\gamma(\text{phenalenyl based superallyl radical})| = 35$ . In contrast, the model ethylene, allyl radical/cation, and butadiene systems with stretched carbon–carbon bond lengths (2.0 Å), having intermediate diradical characters, exhibit similar  $\gamma$  features to those of the phenalenyl based superpolyene systems. This exemplifies that the size dependence of  $\gamma$  as well as its sign change by introducing a positive charge on the phenalenyl based superpolyene systems originate from their intermediate diradical characters. In addition, the change from the lowest to the highest  $\pi$ -electron spin states significantly reduces the  $\gamma$  amplitudes of the neutral phenalenyl based superpolyene systems. For phenalenyl based superallyl cation, the sign inversion of  $\gamma$  (from negative to positive) is observed upon switching between the singlet and triplet states, which is predicted to be associated with a modification of the balance between the positive and negative contributions to  $\gamma$ . The present study paves the way toward designing a variety of open-shell NLO supermolecular systems composed of phenalenyl radical building blocks.



## 1. INTRODUCTION

Since recent theoretical and experimental findings on the intriguing electronic and spin properties of open-shell molecular systems,<sup>1–3</sup> polyaromatic hydrocarbons (PAHs), including graphenes,<sup>1,3–5</sup> have attracted much attention both in chemistry and physics. For instance, the third-order nonlinear optical (NLO) properties, at the molecular level, and the second hyperpolarizability ( $\gamma$ ) of open-shell singlet systems with intermediate diradical characters have been theoretically predicted to exhibit a significant enhancement as compared to conventional closed-shell molecular systems.<sup>6</sup> The validity of this novel structure–property

relationship has been theoretically confirmed using various open-shell singlet models and real compounds including hydrogen molecule and hydrogen chains with various bond lengths,<sup>7</sup> *p*-quinodimethane and twisted ethylene,<sup>8</sup> 1,3-dipoles,<sup>9</sup> diphenalenyl diradicaloids,<sup>10</sup> nanographenes,<sup>11</sup> and transition metal compounds.<sup>12</sup> These results are also supported by recent experimental data on two-photon absorption and third harmonic

Received: June 4, 2011

Revised: July 7, 2011

Published: July 07, 2011

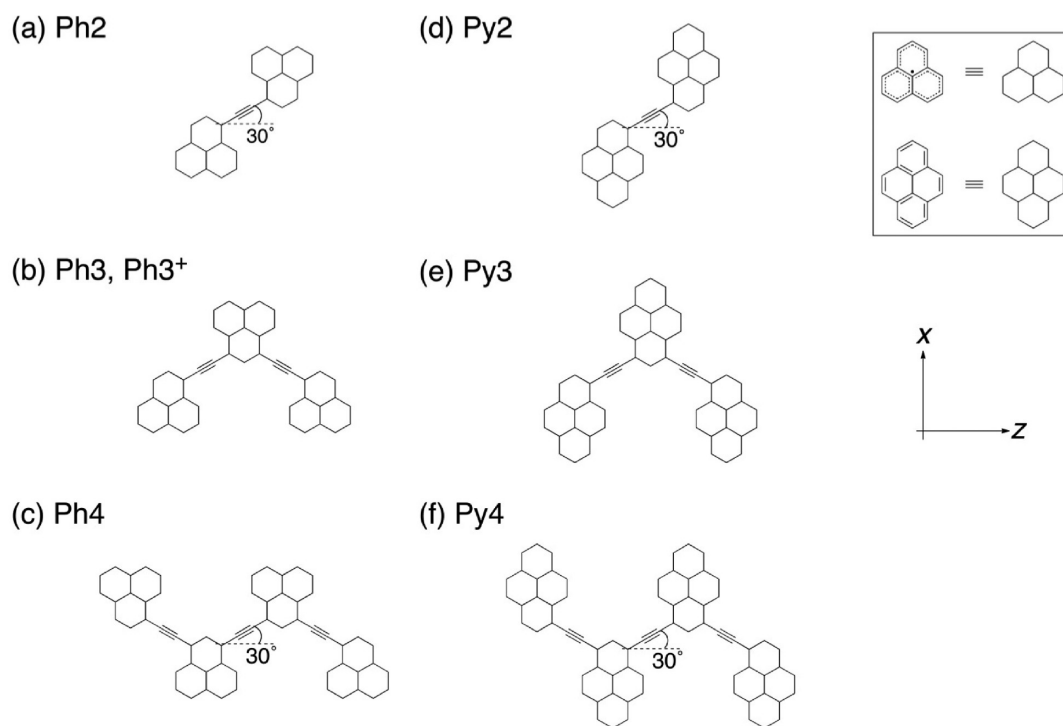


**Figure 1.** Structures of the superpolyene systems composed of acetylene linked phenalenyl [Ph2 (a), Ph3/Ph3<sup>+</sup> (b), Ph4 (c)] and pyrene [Py2 (d), Py3 (e), Py4 (f)] rings. Cartesian axes are also shown. The line connecting both-end carbon atoms of the middle acetylene linker of Ph2, Ph4, Py2, and Py4 forms an angle of 30° with the longitudinal (z) axis. See Supporting Information for optimized geometries.

generation.<sup>13</sup> Indeed, diphenalenyl diradicaloids, *s*-indaceno[1,2,3-*cd*;5,6,7-*c'd'*]diphenalene (IDPL) and dicyclopenta[*b*;g]-naphthaleno[1,2,3-*cd*;6,7,8-*c'd'*]-diphenalene (NDPL), which present intermediate diradical characters, exhibit remarkably large (enhanced by about 2 orders of magnitude) two-photon absorption cross sections as compared to the closed-shell hydrocarbons of similar size.<sup>13a</sup> Other investigations have also evidenced the remarkable linear<sup>14</sup> and nonlinear<sup>15</sup> optical properties of multiradical compounds as well as their vibrational signatures.<sup>16</sup>

In particular, spin-unrestricted hybrid density functional theory (UDFT) calculations have shown that open-shell singlet diphenalenyl diradicaloids involving acetylene  $\pi$ -conjugated linker, that is, 1,2-bis(phenalen-1-ylidene)ethene (BPLE), exhibit a larger (more than twice) longitudinal  $\gamma$  value than its closed-shell analog, that is, bis(pyren-1-yl)ethyne (BPRY), which involves pyrene rings instead of phenalenyl rings and possesses a similar  $\pi$ -conjugation length to BPLE.<sup>10</sup> On the basis of these results, we had speculated promising NLO architectures based on the phenalenyl unit, that is, open-shell super- and supramolecular systems composed of BPLEs.<sup>10a</sup> Although the NLO properties of these systems are expected to be controlled by adjusting the architectures, the diradical characters, and the charge states, there have been no theoretical/experimental studies on these compounds so far due to the difficulty in describing the electronic structures and the NLO properties of such large-size delocalized multiradical systems. In this study, we therefore investigate theoretically open-shell “super-polyene” systems composed of acetylene-linked phenalenyl radicals, that is, superethylene, superallyl radical/cation, and superbutadiene, to clarify the relationships between their diradical characters and static  $\gamma$  values. This is performed by employing the long-range corrected UDFT, LC-UBLYP, method, in which the Hartree–Fock

(HF) exchange term is included in a range-separation manner.<sup>17</sup> As reference closed-shell systems, we examine the analogous superpolyenes composed of acetylene-linked pyrenes as well as regular and model polyenes, that is, ethylene, allyl radical/cation, and butadiene, which have equilibrium and stretched carbon–carbon bond lengths, respectively. The stretching of the carbon–carbon bonds enables to realize model open-shell singlet states with intermediate diradical characters. From comparing their diradical characters and  $\gamma$  values, their structural dependences are clarified as well as the effects of introducing charge and of switching between the ground state singlet and higher spin states. The results obtained in this study provide a new path toward highly efficient and tunable open-shell singlet third-order NLO systems.

## 2. THEORETICAL AND COMPUTATIONAL ASPECTS

### 2.1. Geometrical Structures and Diradical Characters.

Figure 1 displays the structures of superethylenes (Ph2, Py2), superallyls [Ph3, Ph3<sup>+</sup> (cation state), Py3], and superbutadienes, (Ph4, Py4), where “Ph $n$ ” and “Py $n$ ” indicate supermolecules composed of  $n$  phenalenyl or pyrene units and  $n-1$  acetylene linkers. The spin-unrestricted (U)/spin-restricted (R) B3LYP exchange–correlation functional was adopted for the geometry optimizations because it reproduces the experimental structures of conjugated diradical systems<sup>18</sup> as well as those obtained using strongly correlated *ab initio* molecular orbital (MO) methods in the weak and intermediate electron-correlation regimes. The 6-31G\* basis set was employed while the geometries are constrained to be in the XZ plane except for the highest spin (quintet) states of Ph4, which has  $C_1$  symmetry though it presents an almost planar geometry. In addition, systems with 2 or 4 units are constrained to the  $C_{2h}$  symmetry, while those with

3 units are constrained to  $C_{2v}$  symmetry (see Supporting Information). The molecules are oriented so that the line connecting both-end carbon atoms of the middle acetylene linker of Ph2, Ph4, Py2, and Py4 forms an angle of  $30^\circ$  with the longitudinal ( $z$ ) axis. We first examined the lowest spin states of these systems, that is, the singlet states of Ph2 (neutral), Ph3<sup>+</sup> (cation), Ph4 (neutral), Py2 (neutral), Py3 (neutral), and Py4 (neutral), as well as the doublet state for Ph3 (neutral). We next examined the highest spin states of phenalenyl-based systems, that is, Ph2 (triplet, neutral), Ph3 (quartet, neutral), Ph3<sup>+</sup> (triplet, cation), and Ph4 (quintet, neutral), to clarify the spin state dependences of  $\gamma$ . The energy gap between the highest spin (HS) and lowest spin (LS) states,  $E(\text{HS}) - E(\text{LS})$ , is small and amounts to 6.6 (4.6) (Ph2), 10.9 (8.9) (Ph3), 3.9(2.4) (Ph3<sup>+</sup>), 15.9 (13.0) (Ph4) kcal/mol, as determined at the UB3LYP/6-31G\* (LC-UBLYP/6-31G\*) level of approximation using the UB3LYP/6-31G\* optimized geometries. It is here noteworthy to examine the lengths of the acetylene linkers, referred to as linker bonds, in the singlet and the highest spin states from the viewpoint of the bond length alternation observed in regular polyenes. For the singlets, these lengths are 4.000 Å (Ph2), 4.020 Å (Ph3), 4.016 Å (Ph3<sup>+</sup>), 4.016 Å (end, Ph4), 4.033 Å (center, Ph4) versus 4.059 Å (Py2), 4.060 Å (Py3), 4.060 Å (end, Py4), 4.061 Å (center, Py4). Those of the highest spin states are 4.060 Å (triplet Ph2), 4.057 Å (quartet Ph3), 4.030 Å (triplet Ph3<sup>+</sup>), 4.057 Å (end, quintet Ph4), 4.058 Å (center, quintet Ph4). So, (i) the linker-bond lengths of singlet Ph $n$  are smaller than those of singlet Py $n$ , (ii) the linker-bond length of singlet Ph2 is the smallest among the singlet Ph $n$  systems, (iii) a slight linker-bond length alternation is observed between the end and the center linker-bonds of singlet Ph4, and the linker-bond length of singlet Ph3 (which is slightly larger than that of singlet Ph3<sup>+</sup>) is intermediate between them, (iv) the linker-bond lengths of the singlet Py $n$  systems are almost the same and no linker-bond length alternation is observed, (v) except for triplet Ph3<sup>+</sup>, the Ph $n$  systems in the highest spin states exhibit linker-bond lengths, which are larger than those of singlet Ph $n$  but similar to those of singlet Py $n$  systems, and (vi) the linker-bond length of triplet Ph3<sup>+</sup> lies midway between those of singlet Ph3<sup>+</sup> and Py3. These features suggest that the acetylene-linker bonds of singlet Ph $n$  somewhat mimic the behavior of carbon–carbon bonds in singlet polyenes though the linker-bond interactions are much weaker, whereas the linker-bonds of Ph $n$  in the highest spin states and Py $n$  would correspond to the single carbon–carbon bonds of saturated hydrocarbons.

The diradical character ( $y_i$ ) represents the instability of a chemical bond and ranges between 0 (closed-shell) and 1 (pure diradical).<sup>19</sup> It is originally defined in the multiconfigurational self-consistent-field (MC-SCF) theory as twice the weight of the doubly excited configuration in the singlet ground state.<sup>19b</sup> Because we examine multiradical systems with more than two radical sites, like Ph3 and Ph4, multiple diradical characters ( $y_i$ ) have to be considered. To this end, we adopt the following approximate definition (eq 1), which involves the occupation number ( $n_k$ ) of the natural orbitals (NOs) obtained using a spin-unrestricted single-determinant scheme and which can be straightforwardly extended to multiple diradical characters  $y_i$  [related to the highest occupied natural orbital (HONO)- $i$  and the lowest unoccupied natural orbital (LUNO)- $i$ , where  $i = 0, 1, \dots$ ]:

$$y_i = n_{\text{LUNO}+i} = 2 - n_{\text{HONO}-i} \quad (1)$$

The spin-unrestricted single-determinant scheme differs from the spin-restricted single-determinant ones, like RHF or RDFT, where the diradical characters should be all 1 or 0. Indeed, when

considering different orbitals for different spins, the wave function can be expanded in the form of a limited configuration interaction, leading to fractional occupation numbers. To evaluate the multiple diradical characters of the present molecules, we employed the LC-UBLYP/6-31G\* method with a range separating parameter  $\mu = 0.33$ , which is known to provide reliable excitation energies, transition properties, and response properties of closed-shell molecular systems<sup>17</sup> as well as the response properties of open-shell molecular systems.<sup>9</sup> It is here noted that, unlike in UHF calculations, we do not evaluate spin projected diradical characters because the spin contamination effect is smaller in UDFT than in UHF.

**2.2. Second Hyperpolarizability and Hyperpolarizability Density Analysis.** The longitudinal component of the electronic static  $\gamma$ ,  $\gamma_{zzzz}$  was calculated for Ph $n$  and Py $n$  compounds of increasing size by adopting the finite-field approach,<sup>20</sup> which consists in the fourth-order differentiation of the energy with respect to the electric field ( $F$ ):

$$\gamma = \lim_{F \rightarrow 0} \frac{1}{36F^4} [E(3F) - 12E(2F) + 39E(F) - 56E(0) + 39E(-F) - 12E(-2F) + E(-3F)] \quad (2)$$

The LC-UBLYP exchange-correlation functional with  $\mu = 0.33$  was employed because it semiquantitatively reproduces the  $\gamma$  of several open-shell molecules calculated with the highly correlated spin-unrestricted coupled cluster method.<sup>16</sup> Owing to the relatively small basis set dependences of, at least, the longitudinal and dominant  $\gamma$  tensor component in extended  $\pi$ -conjugated systems,<sup>21</sup> the standard 6-31G\* basis set was chosen while for small compounds, the use of extended basis sets including polarization and diffuse functions is required, even for obtaining qualitative  $\gamma$  values.<sup>22</sup> This choice is substantiated by previous studies where the 6-31G\* basis set reproduces within 10% the  $\gamma$  value of IDPL, calculated using the 6-31G\* + diffuse p ( $\zeta = 0.0523$ ) basis set.<sup>23</sup>

The hyperpolarizability density analysis<sup>24a</sup> was also performed to clarify the spatial electronic contribution to  $\gamma$ . From the expansions of the charge density function  $\rho(r, F)$  and of the dipole moment in a power series of the applied electric field  $F$ , the static  $\gamma$  reads

$$\gamma = -\frac{1}{3!} \int r \rho^{(3)}(r) d^3r \quad (3)$$

where

$$\rho^{(3)}(r) = \left. \frac{\partial^3 \rho}{\partial F^3} \right|_{F=0} \quad (4)$$

Here,  $r$  represents the  $z$ -component of the electron coordinate. This third-order derivative of the electron density with respect to the applied electric fields,  $\rho^{(3)}(r)$ , is referred to as the  $\gamma$  density. The positive/negative  $\rho^{(3)}(r)$  values multiplied by  $F^3$  correspond therefore to the third-order field-induced electron density variations, giving rise to the third-order contribution to the dipole moment in the direction from positive to negative  $\gamma$  density. The  $\gamma$  densities are calculated for a grid of points using a numerical third-order differentiation formula of the electron densities. All calculations were performed using the Gaussian 09 program package.<sup>25</sup>

## 3. RESULTS AND DISCUSSION

**3.1. Diradical Character Dependences of  $\gamma$  in Superpolyene Systems in the Lowest Spin States.** First, we examine the diradical characters  $y_0$  and  $y_1$  of the Ph $n$  ( $n = 2, 3, 3^+, 4$ ) and Py $n$



**Table 1. Spin States, Diradical Characters ( $y_0$ ,  $y_1$ ),<sup>a</sup> and  $\gamma$  Values for Open-Shell (Phn) and Closed-Shell (Pyn) Suprapolyene Systems in the Lowest Spin States**

system	spin state	$y_0$	$y_1$	$\gamma [\times 10^4 \text{ a.u.}]$
Ph2	singlet	0.570	0.041	50
Ph3	doublet	0.531	0.044	227
Ph3 <sup>+</sup>	singlet	0.692	0.057	$-8 \times 10^3$
Ph4	singlet	0.752	0.493	525
Py2	singlet	0.0	0.0	12
Py3	singlet	0.0	0.0	27
Py4	singlet	0.0	0.0	46

<sup>a</sup>The  $y_0$  and  $y_1$  values are obtained from the occupation numbers of LUNO and LUNO+1, respectively, calculated by the LC-(U)BLYP/6-31G\* method.

( $n = 2, 3, 4$ ) systems in their lowest spin state. For systems with an even number of units, the use of eq 1 is straightforward. For Ph3,  $y_0$  and  $y_1$  are obtained from the occupation numbers of LUNO and LUNO+1, respectively, where eq 1 is satisfied for (HONO-1, LUNO) and (HONO-2, LUNO+1) because for this doublet case the HONO is the singly occupied natural orbital with an occupation number of 1. The  $y_0$  of Phn ( $n = 2, 3, 3^+, 4$ ) lies in the intermediate region and increases with the number of monomers (Table 1). The  $y_1$  values of Ph2, Ph3, and Ph3<sup>+</sup> are negligible, while that of Ph4 exhibits an intermediate value. This indicates that Ph2 and Ph3<sup>+</sup> are regarded as intermediate diradical systems, Ph3 as an intermediate triradical system, while Ph4 as an intermediate tetraradical system. The intermediate diradical characters of these systems suggest that the radicals of each phenalenyl ring interact with each others with intermediate strength through the acetylene  $\pi$ -conjugated linkers in an antiferromagnetic manner between adjacent phenalenyl rings (both-end phenalenyl rings for Ph3<sup>+</sup>), which results in the delocalization of the radical spins over the whole system. Such prediction of the spin distributions in Phn is exemplified by the Mulliken spin density maps shown in Figure 2. The dominant positive (up) and negative (down) spin densities in Ph2, Ph3, and Ph4 are alternately distributed on the C atoms following Ovchinnikov's rule,<sup>26</sup> resulting in an alternation at the level of the phenalenyl rings (see the sum of the Mulliken spin densities within the dashed circles shown in Figure 2). In contrast to Ph3, in Ph3<sup>+</sup> the spin densities are primarily distributed on the both-end phenalenyl rings. These features are qualitatively understood by their resonance structures (Figure 2). In sharp contrast, all singlet Pyn systems are closed-shell, as expected due to the zero values of  $y_0$  and  $y_1$ , which enables Pyn to play the role of closed-shell references.

We next investigate the  $\gamma$  of these systems. The  $\gamma$  values of Phn are larger than those of Pyn for each  $n$  ( $n = 2-4$ ), and the ratio increases with  $n$ :  $\gamma(\text{Phn})/\gamma(\text{Pyn}) = 4.2$  ( $n = 2$ ), 8.4 ( $n = 3$ ), and 11 ( $n = 4$ ). The  $\gamma$  values exhibit a more striking size dependence for Phn than for Pyn:  $\gamma(n)/\gamma(2) = 4.5$  ( $n = 3$ ) and 11 ( $n = 4$ ) for Phn versus 2.3 ( $n = 3$ ) and 3.8 ( $n = 4$ ) for Pyn. These larger  $\gamma$  amplitudes for open-shell singlet systems with intermediate diradical characters are in agreement with our structure–property relationship.<sup>6</sup> The much smaller size dependence of  $\gamma$  for Pyn than for Phn also indicates the negligible  $\pi$ -electron delocalization over the pyrene rings and acetylene linkers in Pyn systems. This latter point is also consistent with the same linker-bond lengths in Pyn systems (see section 2.1). The introduction of positive charge into Ph3

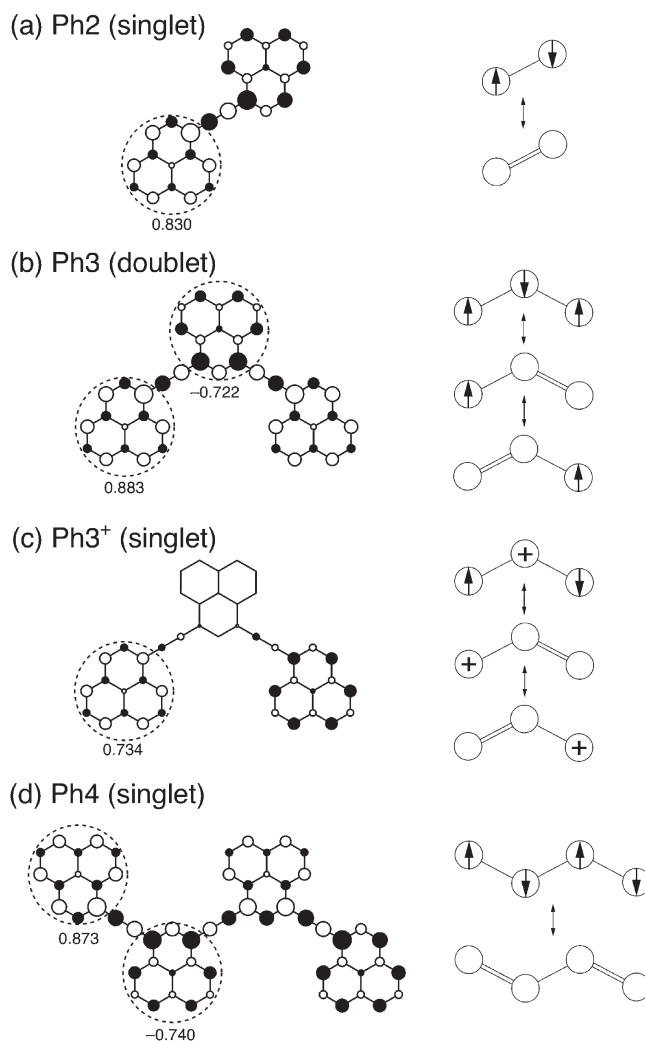


**Figure 2.** Mulliken spin density distributions (positive: white circle, negative: black circle) for Ph2 (singlet), Ph3 (doublet), Ph3<sup>+</sup> (singlet), and Ph4 (singlet) calculated using the LC-UBLYP/6-31G\* method and the sums of Mulliken spin densities inside the dashed circles. The corresponding resonance structures are also shown, where the white circle, arrow, and connection line schematically indicate the phenalenyl moiety, total spin on the phenalenyl ring, and a bond between the up and down spins, respectively.

(suprallyl radical), that is, the removal of an electron, causes a change of sign and a remarkable (35 times) enhancement of  $\gamma$  relative to Ph3. This change of sign can be interpreted by referring to the summation-overstate (SOS) expression of  $\gamma$ .<sup>7a,24</sup> Indeed, in the case of symmetric systems,  $\gamma$  can be partitioned into the two types of contributions (type II and III-2):<sup>24</sup>

$$\gamma = \gamma^{\text{II}} + \gamma^{\text{III-2}} = -4 \sum_{n,m} \frac{(\mu_{n0})^2 (\mu_{m0})^2}{E_{n0} E_{m0}^2} + 4 \sum_{\substack{n',m,n=1 \\ (n' \neq m, m \neq n)}} \frac{\mu_{0n'} \mu_{nm} \mu_{mn'} \mu_{n'0}}{E_{n0} E_{m0} E_{n'0}} \quad (5)$$

where  $\mu_{n0}$  is the transition moment between the ground (0) and the  $n$ th excited states,  $\mu_{nm}$  is the transition moment between the  $n$ th

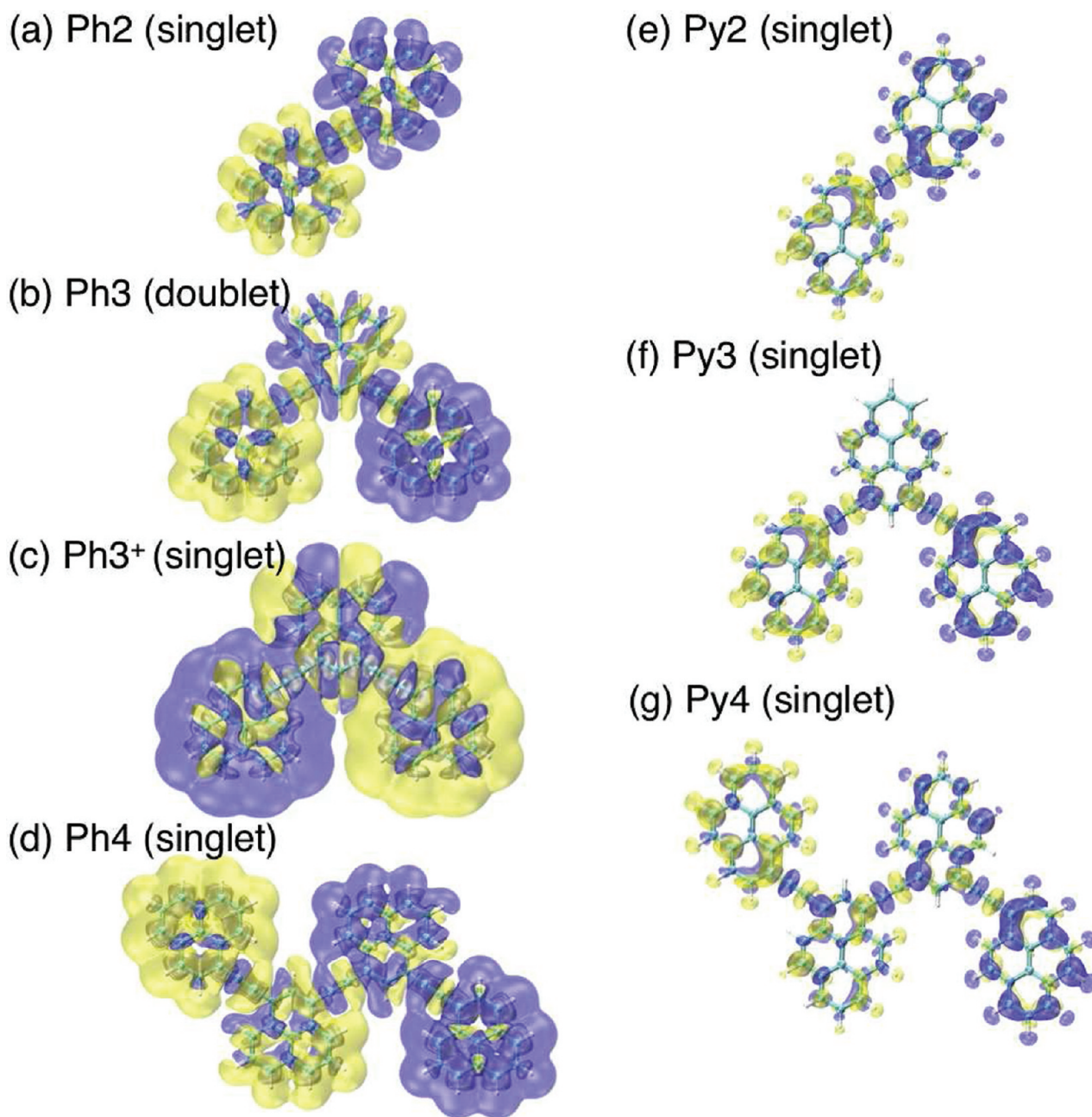


**Figure 3.**  $\gamma_{zzzz}$  density distributions of Ph2 (singlet) (a), Ph3 (doublet) (b), Ph3<sup>+</sup> (singlet; c), Ph4 (singlet; d), Py2 (singlet; e), Py3 (singlet; f), and Py4 (singlet; g) calculated using the LC-(U)BLYP/6-31G\* method. The yellow and blue surfaces represent positive and negative densities, respectively, with iso-surfaces of  $\pm 100$  a.u.

and the  $m$ th excited states, and  $E_{n0}$  is the transition energy given by  $(E_n - E_0)$ . Each fourth-order virtual excitation process  $(0-i-j-k-0)$  contributing to  $\gamma$  corresponds to a series of subscripts in the numerator of eq 5, as illustrated in Figure 1S in the Supporting Information. As seen from eq 5, the type II  $(0-n-0-m-0)$  process, which involves the ground state (0) in the middle of the virtual excitation path, gives negative contributions, while the total type III-2  $(0-n-m-n'-0)$  contributions is usually positive because the dominant diagonal  $(0-n-m-n-0)$  terms are positive definite. Thus, the magnitude and the sign of  $\gamma$  for symmetric systems are determined by the competition between type II and type III-2 contributions. Indeed, for the allyl cation, the negative type II contribution

overcomes the positive type III-2 contribution.<sup>24c</sup> Moreover, the remarkable enhancement of the  $\gamma$  amplitude of Ph3<sup>+</sup> is caused by the intermediate diradical characters. This analysis is further clarified by examining several open-shell allyl models in the next section.

Figure 3 shows the  $\gamma$  density distributions for Ph $n$  and Py $n$  in their lowest spin states. For all systems, the  $\pi$ -electron contributions are dominant. For Ph2, Ph3, and Ph4, extended positive and negative  $\gamma$  densities primarily distributed on the phenalenyl rings are well separated on the left- and right-hand sides, leading to large positive contributions to  $\gamma$ . In contrast, Py2, Py3, and Py4 show much smaller  $\gamma$  density amplitudes, though the

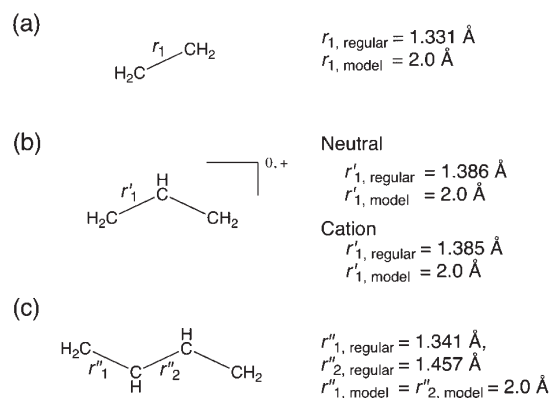


**Figure 4.** Geometrical structures of the optimized (regular) and stretched (model) polyene systems [ $\text{C}_2\text{H}_4$  (singlet; a),  $\text{C}_3\text{H}_5$  (doublet; b),  $\text{C}_3\text{H}_5^+$  (singlet; b),  $\text{C}_4\text{H}_6$  (singlet; c)]. See also the caption of Figure 1 and Supporting Information.

**Table 2.** Spin States, Diradical Characters ( $y_0, y_1$ ),<sup>a</sup> and  $\gamma$  Values for Polynene Systems ( $\text{C}_2\text{H}_4$ ,  $\text{C}_3\text{H}_5$ ,  $\text{C}_3\text{H}_5^+$ ,  $\text{C}_4\text{H}_6$ ) with Regular and Model Geometries<sup>a</sup> in the Lowest Spin States

system	spin state	geometry	$y_0$	$y_1$	$\gamma$ [a.u.]
$\text{C}_2\text{H}_4$	singlet	regular	0.0	0.0	53
		model	0.509	0.009	946
$\text{C}_3\text{H}_5$	doublet	regular	0.0	0.0	509
		model	0.374	0.009	3290
$\text{C}_3\text{H}_5^+$	singlet	regular	0.0	0.0	−308
		model	0.527	0.003	$-14.4 \times 10^4$
$\text{C}_4\text{H}_6$	singlet	regular	0.0	0.0	1760
		model	0.676	0.321	8100

<sup>a</sup>The “regular” and “model” mean the geometries optimized by the LC-(U)B3LYP/6-31G\* method and those replaced by the stretched carbon–carbon bond length (2.0 Å), respectively.

positive and negative  $\gamma$  density distributions are also separated on both sides. For  $\text{Ph}_3^+$ , enhanced  $\gamma$  densities are observed, particularly on the both-end phenalenyl rings, while a significant cancellation between positive and negative  $\gamma$  densities occurs in the central phenalenyl ring. The separation of the positive and negative dominant  $\gamma$  densities in  $\text{Ph}_3^+$  coincides with the dominant spin polarization region (see Figure 2), which substantiates the direct link between the intermediate diradical character and the enhancement of  $\gamma$ .

**3.2. Comparison of Diradical Character and  $\gamma$  between Phenalenyl Based Open-Shell Superpolyene and Polyene Systems in their Lowest Spin States.** To investigate the similarities between phenalenyl based open-shell superpolyene systems [superethylene ( $\text{Ph}_2$ ), superallyl ( $\text{Ph}_3$ ,  $\text{Ph}_3^+$ ), and superbutadiene ( $\text{Ph}_4$ )] and polyene systems [ethylene ( $\text{C}_2\text{H}_4$ ), allyl radical/cation ( $\text{C}_3\text{H}_5/\text{C}_3\text{H}_5^+$ ), and butadiene ( $\text{C}_4\text{H}_6$ )] in their lowest spin states, we examine two series of polyene systems, (i) the regular polyenes with optimized geometries and (ii) model polyenes having stretched carbon–carbon bond lengths (2.0 Å; see Figure 4 as well as Supporting Information). The geometries of  $\text{C}_3\text{H}_5$  and  $\text{C}_3\text{H}_5^+$  belong to  $\text{C}_{2v}$  symmetry, while those of  $\text{C}_2\text{H}_4$  and  $\text{C}_4\text{H}_6$  belong to  $\text{C}_{2h}$  symmetry, and the line connecting their middle carbon atoms forms an angle of  $30^\circ$  with the longitudinal

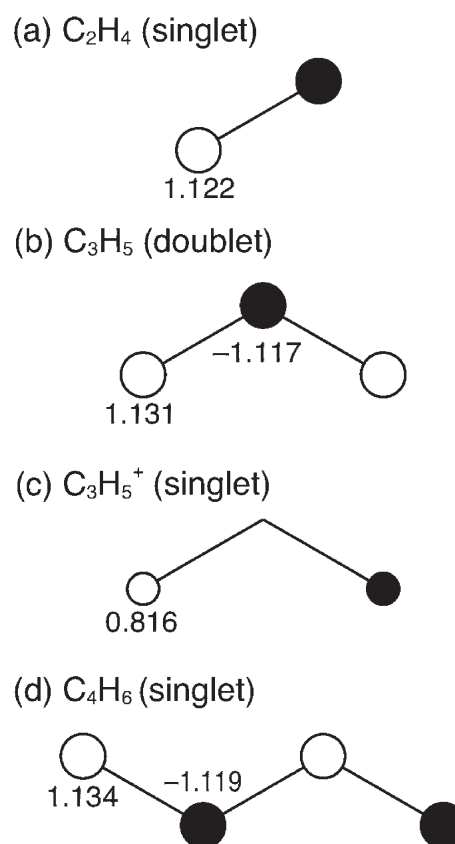


**Figure 5.** Mulliken spin density distributions (positive: white circle, negative: black circle) of the stretched  $\text{C}_2\text{H}_4$  (singlet; a),  $\text{C}_3\text{H}_5$  (doublet; b),  $\text{C}_3\text{H}_5^+$  (singlet; c), and  $\text{C}_4\text{H}_6$  (singlet; d) calculated using the LC-UBLYP/6-31G\* method.

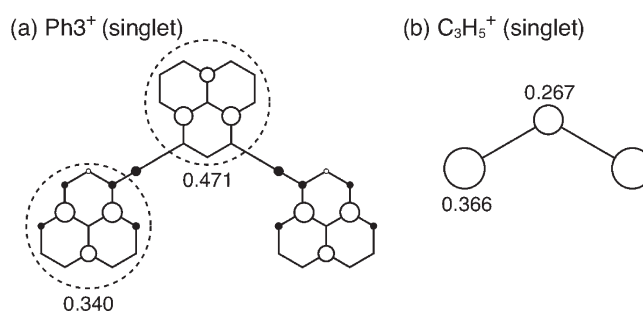


**Figure 6.** Mulliken net charge density distributions (positive: white circle, negative: black circle) of  $\text{Ph}_3^+$  (singlet) and model  $\text{C}_3\text{H}_5^+$  (singlet) calculated using the LC-UBLYP/6-31G\* method. The sums of the Mulliken net charge densities inside the dashed circles are also shown.

(z) axis. Their spin states, diradical characters ( $y_0$  and  $y_1$ ), and  $\gamma$  values (diagonal z component) are listed in Table 2. The regular polyenes are closed-shell singlets, except  $\text{C}_3\text{H}_5$ , which is a doublet, while the stretched ones are the open-shell systems with intermediate diradical characters. Figures 5 and 6 show the Mulliken spin and net charge densities for these model systems. The alternant spin density patterns as well as the net charge distribution match to some extent (the relative amplitudes on the



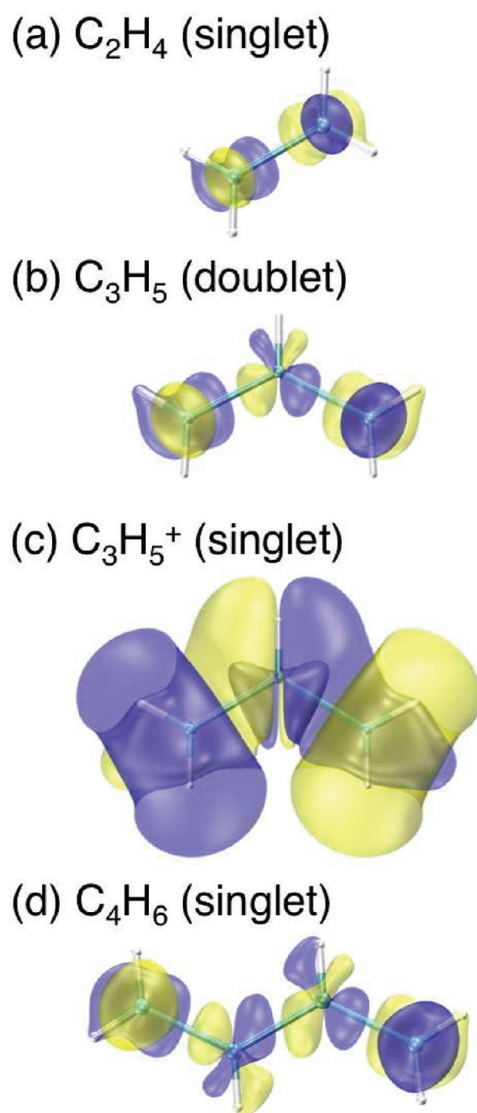


**Figure 7.**  $\gamma_{zzzz}$  density distributions for the stretched  $C_2H_4$  (singlet; a),  $C_3H_5$  (doublet; b),  $C_3H_5^+$  (singlet; c), and  $C_4H_6$  (singlet; d) systems calculated using the LC-UBLYP/6-31G\* method. The yellow and blue surfaces represent positive and negative densities, respectively, with iso-surfaces of  $\pm 50$  a.u.

inner and outer rings/atoms are inverted) those of the open-shell superpolyene systems  $Ph_n$ . Therefore, these model polyene systems are expected to display analogous  $\gamma$  features to those of the superpolyene systems. Indeed, the  $\gamma$  values are in the 1:3.5:8.6 ratio for the stretched  $C_2H_4$ ,  $C_3H_5$ , and  $C_4H_6$ , in comparison to 1:4.5:11 for the corresponding  $Ph_n$ . Nevertheless, owing to their much different size (or number of  $\pi$ -electrons), the  $\gamma$  values of the model systems are much smaller than those of superpolyenes. Also in agreement with  $Ph_3^+$ , the  $C_3H_5^+$  cation shows a negative  $\gamma$  value with a large amplitude, which is 44 times as large as that of the model  $C_3H_5$  radical (cf. 35 times for  $Ph_3^+/Ph_3$ ). In contrast, the  $\gamma$  values of the regular polyenes are in the 1:9.6:33 ratio for  $C_2H_4$ :  $C_3H_5$ :  $C_4H_6$ , which exhibits a larger size dependence than the model polyene systems, whereas the  $\gamma$  amplitudes are smaller. Such larger size dependence of the  $\gamma$  in closed-shell  $\pi$ -conjugated chains coincides with previous results

**Table 3.**  $\gamma$  Values for Open-Shell Superpolyene ( $Ph_n$ ) and Model Polyene Systems [with Stretched Carbon–Carbon Bond Length (2.0 Å)] in the Highest Spin States<sup>a</sup>

superpolyene systems	spin state	$\gamma [\times 10^4 \text{ a.u.}]$
Ph2	triplet	13
Ph3	quartet	43
Ph3 <sup>+</sup>	triplet	$14.4 \times 10^3$
Ph4	quintet	86
model polyene systems	spin state	$\gamma [\text{a.u.}]$
$C_2H_4$	triplet	125
$C_3H_5$	quartet	365
$C_3H_5^+$	triplet	5920
$C_4H_6$	quintet	1380

<sup>a</sup> The diradical characters  $y_0$  and  $y_1$ , obtained from the occupation numbers of LUNO and LUNO+1, respectively, of these highest spin state systems calculated by the LC-UBLYP/6-31G\* method, are found to be zero.

on hydrogen chains.<sup>7b</sup> On the other hand, the  $\gamma$  of regular  $C_3H_5^+$  is negative like that of  $Ph_3^+$ , but its ratio with respect to the neutral radical is much smaller than that of the model  $C_3H_5$ :  $|\gamma(\text{regular } C_3H_5^+)/\gamma(\text{regular } C_3H_5)| = 0.61$  versus  $|\gamma(\text{model } C_3H_5^+)/\gamma(\text{model } C_3H_5)| = 44$ . Such remarkable enhancement of  $\gamma$  in open-shell cation radical systems are predicted to be caused by the enhancement of type II contribution, which is ascribed to the significant reduction of the first excitation energy in the intermediate and large diradical character regions.<sup>6a</sup> Figure 7 shows the  $\gamma$  density distributions of the model polyene systems. Their topology and the relative amplitudes of the dominant  $\pi$ -electron  $\gamma$  density distributions on the carbon atom sites are qualitatively similar to those on phenalenyl rings of the corresponding  $Ph_n$ . This mapping between the open-shell  $Ph_n$  and model polyene systems substantiates that the sign, the amplitude, and the size dependence of  $\gamma$  in these open-shell linear conjugated systems is governed by their diradical characters.

**3.3. Spin State Dependences of  $\gamma$  in Phenalenyl Based Open-Shell Superpolyene and Their Model Polyene Systems.** Table 3 lists the  $\gamma$  values of the  $\pi$ -electron highest spin states of the  $Ph_n$  systems as well as those of the stretched polyenes having the same geometries (CC bond lengths of 2.0 Å) as in the lowest spin state. Except for cationic  $Ph_3^+$ , the  $\gamma$  amplitudes are much smaller than those in the lowest spin state:  $\gamma(\text{highest multiplet})/\gamma(\text{singlet}) = 0.26$  ( $Ph_2$ ), 0.19 ( $Ph_3$ ), and 0.16 ( $Ph_4$ ). This feature coincides with our structure–property relationship:<sup>10b</sup> commuting from the singlet to the highest multiplet in open-shell singlet systems with intermediate diradical characters leads to a significant reduction of  $\gamma$ . For the cationic  $Ph_3^+$ , the sign of  $\gamma$  is inverted with respect to its singlet analog and its amplitude is 1.8 times enhanced. For the model polyene systems, a similar  $\gamma$  reduction is observed with  $\gamma(\text{highest multiplet})/\gamma(\text{singlet})$  ratios of 0.13 ( $C_2H_4$ ), 0.11 ( $C_3H_5$ ), and 0.17 ( $C_4H_6$ ), while for  $C_3H_5^+$ ,  $\gamma$  changes sign but it is also significantly reduced. In general, negative  $\gamma$  values in symmetric systems originate from slight differences between positive (type III-2) and negative (type II) contributions, both of which having large amplitudes.<sup>24</sup> The change in sign of  $\gamma$  is thus predicted to be caused by the relative reduction of the negative type II contribution because the polarization between parallel spins is attenuated due to the Pauli principle as compared to the case of



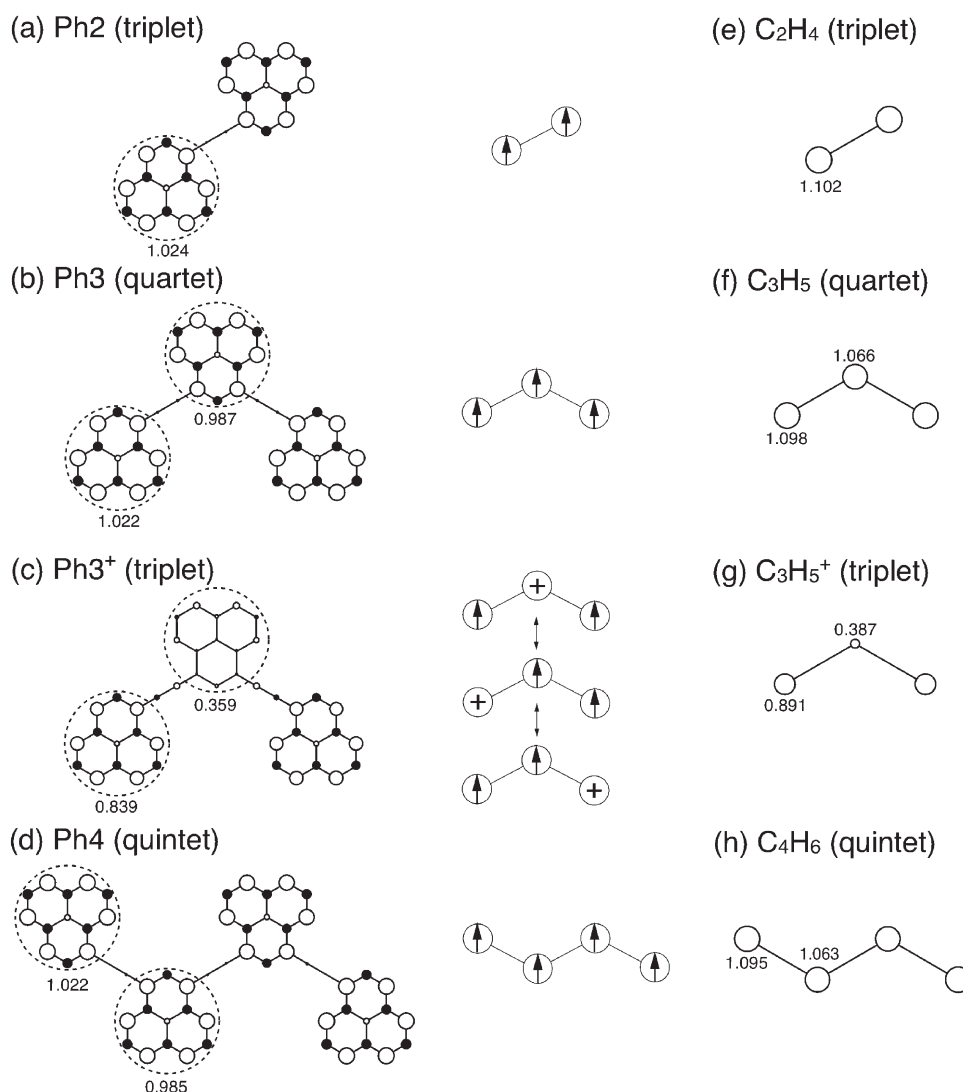


**Figure 8.** Mulliken spin density distributions (positive: white circle, negative: black circle) for Ph<sub>2</sub> (triplet; a), Ph<sub>3</sub> (quartet; b), Ph<sub>3</sub><sup>+</sup> (triplet; c), and Ph<sub>4</sub> (quintet; d) as well as for the stretched C<sub>2</sub>H<sub>4</sub> (triplet; e), C<sub>3</sub>H<sub>5</sub> (quartet; f), C<sub>3</sub>H<sub>5</sub><sup>+</sup> (triplet; g), and C<sub>4</sub>H<sub>6</sub> (quintet; h) systems calculated using the LC-UBLYP/6-31G\* method. See also the caption of Figure 2.

singlet diradical systems with antiparallel spins. Consequently, besides this qualitative explanation, the relative  $\gamma$  amplitudes for C<sub>3</sub>H<sub>5</sub><sup>+</sup> and Ph<sub>3</sub><sup>+</sup> in their singlet and triplet state are difficult to further interpret. Figure 8 evidences that for Ph<sub>2</sub>–Ph<sub>4</sub> the spin densities are distributed with almost one parallel spin per phenalenyl ring, while for cationic Ph<sub>3</sub><sup>+</sup> the sum of spin density amplitudes in the central phenalenyl ring is significantly reduced due to charging, which contributes to the enhancement of the polarization between both-end and central ring regions. Similar spin density distributions are also observed in the model polyene systems. Though their amplitudes are reduced, the topology of  $\gamma$  density distributions (Figure 9) of the highest spin states of neutral Ph<sub>*n*</sub> is similar to this of their ground states. In contrast, for cationic triplet Ph<sub>3</sub><sup>+</sup>, the dominant contributions, which come from both-end phenalenyl rings, have the opposite sign with respect to the singlet state. The same topology relation between the lowest and the highest spin states is also observed in model polyenes though for C<sub>4</sub>H<sub>6</sub> (quintet) the cancellation between positive and negative contributions to  $\gamma$  is more obvious.

#### 4. CONCLUDING REMARKS

In this study, we have investigated the relationship between the diradical characters and the longitudinal second hyperpolarizabilities  $\gamma$  of superpolyene systems composed of acetylene-linked phenalenyl/pyrene rings. The phenalenyl-based superethylene, superallyl, and superbutadiene in their lowest spin states have intermediate diradical characters and exhibit larger  $\gamma$  values than the closed-shell pyrene-based superpolyene systems. The introduction of a positive charge into the phenalenyl based superallyl radical changes the sign of  $\gamma$  and enhances its amplitude by a factor of 35. Although such sign inversion is also observed in the allyl radical and cation systems in their ground state equilibrium geometries, the relative amplitude of  $\gamma$  is much different, that is,  $|\gamma(\text{regular allyl cation})/\gamma(\text{regular allyl radical})| = 0.61$  versus  $|\gamma(\text{superallyl cation})/\gamma(\text{superallyl radical})| = 35$ . In contrast, the model ethylene, allyl radical/cation, and butadiene systems with stretched carbon–carbon bond lengths (2.0 Å), having intermediate diradical characters, exhibit similar  $\gamma$  features to those of the phenalenyl-based superpolyene systems.

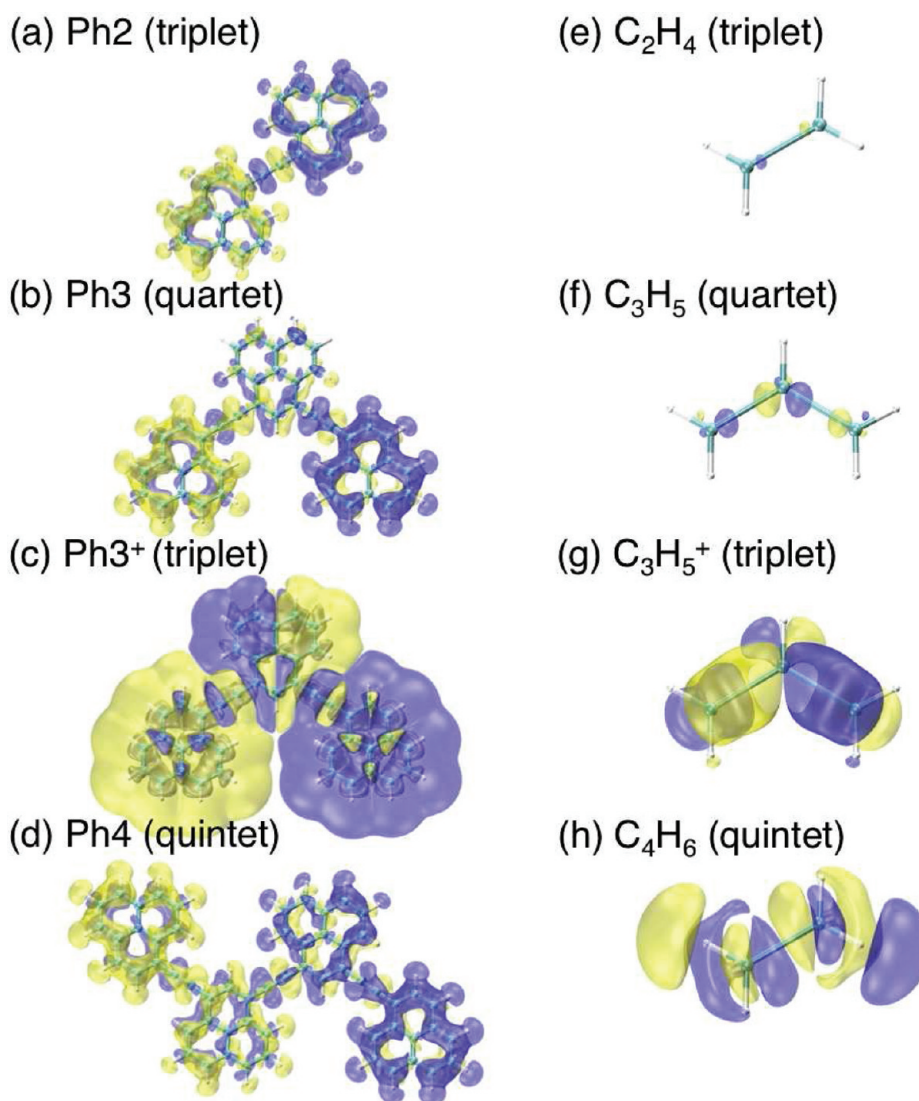


**Figure 9.**  $\gamma_{zzzz}$  density distributions for Ph2 (triplet; a), Ph3 (quartet; b), Ph3<sup>+</sup> (triplet; c), and Ph4 (quintet; d) as well as for the stretched C<sub>2</sub>H<sub>4</sub> (triplet; e), C<sub>3</sub>H<sub>5</sub> (quartet; f), C<sub>3</sub>H<sub>5</sub><sup>+</sup> (triplet; g), and C<sub>4</sub>H<sub>6</sub> (quintet; h) systems calculated using the LC-UBLYP/6-31G\* method. The yellow and blue surfaces represent positive and negative densities, respectively, with iso-surfaces of  $\pm 100$  a.u. for Ph $n$  and  $\pm 50$  a.u. for model polyenes.

This exemplifies that the size dependence of  $\gamma$  as well as its sign change by introducing a positive charge on the phenalenyl-based superpolyene systems originate from their intermediate diradical characters. In addition, the change from the lowest to the highest  $\pi$ -electron spin states significantly reduces the  $\gamma$  amplitudes of the neutral Ph $n$  systems, which is in agreement with our previous results.<sup>10b</sup> For cationic Ph3<sup>+</sup>, the sign inversion of  $\gamma$  (from negative to positive) is observed upon switching between the singlet and triplet states, which is predicted to be associated with a modification of the balance between the positive and negative contributions to  $\gamma$ . Note that the model polyene systems with intermediate diradical characters and large  $\gamma$  values are unrealistic systems, while the phenalenyl-based superpolyene systems are more realistic, though they have not been synthesized yet. Nevertheless, these results reveal that such open-shell supermolecular systems composed of acetylene-linked phenalenyl radicals constitute a novel path to design highly efficient and tunable nonlinear optical materials through the control of the open-shell characters and spin states.

## ■ ASSOCIATED CONTENT

**S Supporting Information.** Cartesian coordinates of superpolyenes (Ph2, Ph3, Ph3<sup>+</sup>, Ph4, Py2, Py3, Py4) and regular polyenes (C<sub>2</sub>H<sub>4</sub>, C<sub>3</sub>H<sub>5</sub>, C<sub>3</sub>H<sub>5</sub><sup>+</sup>, C<sub>4</sub>H<sub>6</sub>) optimized by the (U)B3LYP/6-31G\* method as well as those of model polyenes [ $R(C-C) = 2.0$  Å]. Virtual excitation processes, types II and III-2, in  $\gamma$  for symmetric systems based on the SOS formula. This material is available free of charge via the Internet at <http://pubs.acs.org>.

## ■ AUTHOR INFORMATION

### Corresponding Author

\*Fax: +81-6-6850-6268. E-mail: [mnaka@cheng.es.osaka-u.ac.jp](mailto:mnaka@cheng.es.osaka-u.ac.jp).

## ■ ACKNOWLEDGMENT

This work was supported by Grant-in-Aid for Scientific Research (No. 21350011) and “Japan–Belgium Cooperative

Program” (J091102006) from Japan Society for the Promotion of Science (JSPS), and the global COE (center of excellence) program “Global Education and Research Center for Bio-Environmental Chemistry” of Osaka University. Theoretical calculations were partly performed using the Research Center for Computational Science, Okazaki, Japan. This work has also been supported by the Academy Louvain (ARC “Extended- $\pi$ -Conjugated Molecular Tinkertoys for Optoelectronics, and Spintronics”) and by the Belgian Government (IUAP No P06-27 “Functional Supramolecular Systems”).

## REFERENCES

- (1) (a) Lambert, C. *Angew. Chem., Int. Ed.* **2011**, *50*, 1756. (b) Du, A.; Smith, S. C. *J. Phys. Chem. Lett.* **2011**, *2*, 73.
- (2) (a) Lahti, P. M.; Ichimura, A. S.; Sanborn, J. A. *J. Phys. Chem. A* **2001**, *105*, 251. (b) Matsuda, K.; Irie, M. *Chem.—Eur. J.* **2001**, *7*, 3466. (c) Scheschkewitz, D.; Amii, H.; Gomitzka, H.; Schoeller, W. W.; Bourissou, D.; Bertrand, G. *Science* **2002**, *295*, 1880. (d) Cui, C.; Brynda, M.; Olmstead, M. M.; Power, P. P. *J. Am. Chem. Soc.* **2004**, *126*, 6510. (e) Ito, A.; Urabe, M.; Tanaka, K. *Angew. Chem., Int. Ed.* **2007**, *46*, 3300.
- (3) (a) Bendikov, M.; Duong, H. M.; Starkey, K.; Houk, K. N.; Carter, E. A.; Wudl, F. *J. Am. Chem. Soc.* **2004**, *126*, 7416. (g) Erratum: *J. Am. Chem. Soc.*, **2004**, *126*, 10493. (b) Hachmann, J.; Dorando, J. J.; Avilés, M.; Chan, G. K.-L. *J. Chem. Phys.* **2007**, *127*, 134309. (c) Jiang, D. E.; Sumpter, B. G.; Dai, S. J. *Chem. Phys.* **2007**, *127*, 124703. (d) Jiang, D. E.; Dai, S. J. *J. Phys. Chem. A* **2008**, *112*, 332. (e) Tönshoff, C.; Bettinger, H. F. *Angew. Chem., Int. Ed.* **2010**, *49*, 4125. (f) Castro Neto, A. H.; Guinea, F.; Peres, N. M. R.; Novoselov, K. S.; Geim, A. K. *Rev. Mod. Phys.* **2009**, *81*, 109.
- (4) (a) Kubo, T.; Shimizu, A.; Uruichi, M.; Yakushi, K.; Nakano, M.; Shiomi, D.; Sato, K.; Takui, T.; Morita, Y.; Nakasuji, K. *Org. Lett.* **2007**, *9*, 81. (b) Huang, J.; Kertesz, M. *J. Am. Chem. Soc.* **2007**, *129*, 1634. (c) Shimizu, A.; Uruichi, M.; Yakushi, K.; Matsuzaki, H.; Okamoto, H.; Nakano, M.; Hirao, Y.; Matsumoto, K.; Kurata, H.; Kubo, T. *Angew. Chem., Int. Ed.* **2009**, *48*, 5482.
- (5) Konishi, A.; Hirao, Y.; Nakano, M.; Shimizu, A.; Botek, E.; Champagne, B.; Shiomi, D.; Sato, K.; Takui, T.; Matsumoto, K.; Kurata, H.; Kubo, T. *J. Am. Chem. Soc.* **2010**, *132*, 11021.
- (6) (a) Nakano, M.; Kishi, R.; Ohta, S.; Takahashi, H.; Kubo, T.; Kamada, K.; Ohta, K.; Botek, E.; Champagne, B. *Phys. Rev. Lett.* **2007**, *99*, 033001. (b) Nakano, M.; Yoneda, K.; Kishi, R.; Takahashi, H.; Kubo, T.; Kamada, K.; Ohta, K.; Botek, E.; Champagne, B. *J. Chem. Phys.* **2009**, *131*, 114316. (c) Nakano, M.; Champagne, B.; Botek, E.; Ohta, K.; Kamada, K.; Kubo, T. *J. Chem. Phys.* **2010**, *133*, 154302.
- (7) (a) Nakano, M.; Kishi, R.; Ohta, S.; Takebe, A.; Takahashi, H.; Furukawa, S.; Kubo, T.; Morita, Y.; Nakasuji, K.; Yamaguchi, K.; Kamada, K.; Ohta, K.; Champagne, B.; Botek, E. *J. Chem. Phys.* **2006**, *125*, 074113. (b) Nakano, M.; Takebe, A.; Kishi, R.; Ohta, S.; Nate, M.; Kubo, T.; Kamada, K.; Ohta, K.; Champagne, B.; Botek, E.; Takahashi, H.; Furukawa, S.; Morita, Y.; Nakasuji, K. *Chem. Phys. Lett.* **2006**, *432*, 473. (c) Takebe, A.; Nakano, M.; Kishi, R.; Nate, M.; Takahashi, H.; Kubo, T.; Kamada, K.; Ohta, K.; Champagne, B.; Botek, E. *Chem. Phys. Lett.* **2008**, *451*, 111.
- (8) Nakano, M.; Kishi, R.; Nitta, T.; Kubo, T.; Nakasuji, K.; Kamada, K.; Ohta, K.; Champagne, B.; Botek, E.; Yamaguchi, K. *J. Phys. Chem. A* **2005**, *109*, 885.
- (9) Kishi, R.; Bonness, S.; Yoneda, K.; Takahashi, H.; Nakano, M.; Botek, E.; Champagne, B.; Kubo, T.; Kamada, K.; Ohta, K.; Tsuneda, T. *J. Chem. Phys.* **2010**, *132*, 094107.
- (10) (a) Ohta, S.; Nakano, M.; Kubo, T.; Kamada, K.; Ohta, K.; Kishi, R.; Nakagawa, N.; Champagne, B.; Botek, E.; Umezaki, S.; Takebe, A.; Takahashi, H.; Furukawa, S.; Morita, Y.; Nakasuji, K.; Yamaguchi, K. *Chem. Phys. Lett.* **2006**, *420*, 432. (b) Ohta, S.; Nakano, M.; Kubo, T.; Kamada, K.; Ohta, K.; Kishi, R.; Nakagawa, N.; Champagne, B.; Botek, E.; Takebe, A.; Umezaki, S.; Nate, M.; Takahashi, H.; Furukawa, S.; Morita, Y.; Nakasuji, K.; Yamaguchi, K. *J. Phys. Chem. A* **2007**, *111*, 3633.
- (11) (a) Nakano, M.; Nagai, H.; Fukui, H.; Yoneda, K.; Kishi, R.; Takahashi, H.; Shimizu, A.; Kubo, T.; Kamada, K.; Ohta, K.; Champagne, B.; Botek, E. *Chem. Phys. Lett.* **2008**, *467*, 120. (b) Nagai, H.; Nakano, M.; Yoneda, K.; Kishi, R.; Takahashi, H.; Shimizu, A.; Kubo, T.; Kamada, K.; Ohta, K.; Botek, E.; Champagne, B. *Chem. Phys. Lett.* **2010**, *489*, 212. (c) Yoneda, K.; Nakano, M.; Fukui, H.; Minami, T.; Shigeta, Y.; Kubo, T.; Botek, E.; Champagne, B. *ChemPhysChem* **2011**, *12*, 1697.
- (12) Fukui, H.; Shigeta, Y.; Nakano, M.; Kubo, T.; Kamada, K.; Ohta, K.; Champagne, B.; Botek, E. *J. Phys. Chem. A* **2011**, *115*, 1117.
- (13) (a) Kamada, K.; Ohta, K.; Kubo, T.; Shimizu, A.; Morita, Y.; Nakasuji, K.; Kishi, R.; Ohta, S.; Furukawa, S.; Takahashi, H.; Nakano, M. *Angew. Chem., Int. Ed.* **2007**, *46*, 3544. (b) Kishida, H.; Hibino, K.; Nakamura, A.; Kato, D.; Abe, J. *Thin Solid Films* **2010**, *519*, 1028.
- (14) (a) Paci, I.; Jonhson, J. C.; Chen, X.; Rana, G.; Popovic, D.; David, D. E.; Nozik, A. J.; Ratner, M. A.; Michl, J. *J. Am. Chem. Soc.* **2006**, *128*, 16546. (b) Train, C.; Norel, L.; Baumgarten, M. *Coord. Chem. Rev.* **2009**, *253*, 2342. (c) Kamada, K.; Ohta, K.; Shimizu, A.; Kubo, T.; Kishi, R.; Takahashi, H.; Botek, E.; Champagne, B.; Nakano, M. *J. Phys. Chem. Lett.* **2010**, *1*, 937. (d) Ponce Ortiz, R.; Casado, J.; Gonzalez, S. R.; Hernandez, V.; Lopez Navarrete, J. T.; Viruela, P. M.; Orti, E.; Takimya, K.; Otsubo, T. *Chem.—Eur. J.* **2010**, *16*, 470. (e) Trinquier, G.; Suaud, N.; Malrieu, J. P. *Chem.—Eur. J.* **2010**, *16*, 8762. (f) Tian, Y. H.; Kertesz, M. *J. Am. Chem. Soc.* **2010**, *132*, 10648. (g) Kishi, R.; Nakano, M. *J. Phys. Chem. A* **2011**, *115*, 3565.
- (15) (a) Hu, W.; Ma, H.; Liu, C.; Jiang, Y. *J. Chem. Phys.* **2007**, *126*, 044903. (b) Yesudas, K.; Bhanuprakash, K. *J. Phys. Chem. A* **2007**, *111*, 1943. (c) Srinivas, K.; Prabhakar, Ch.; Devi, C. L.; Yesudas, K.; Bhanuprakash, K.; Rao, V. J. *J. Phys. Chem. A* **2007**, *111*, 3378. (d) Thomas, A.; Srinivas, K.; Prabhakar, Ch.; Bhanuprakash, K.; Rao, V. J. *Chem. Phys. Lett.* **2008**, *454*, 36. (e) Qiu, Y. Q.; Fan, H. L.; Sun, S. L.; Liu, C. G.; Su, Z. M. *J. Phys. Chem. A* **2008**, *112*, 83. (f) Li, Z. J.; Wang, F. F.; Li, Z. R.; Xu, H. L.; Huang, X. R.; Wu, D.; Chen, W.; Yu, G. T.; Gu, F. L.; Aoki, Y. *Phys. Chem. Chem. Phys.* **2009**, *11*, 402. (g) Jha, P. C.; Rinkevicius, Z.; Ågren, H. *ChemPhysChem* **2009**, *10*, 817. (h) Serrano-Andrés, L.; Avramopoulos, A.; Li, J.; Labéguerie, P.; Bégue, D.; Kellö, V.; Papadopoulos, M. G. *J. Chem. Phys.* **2009**, *131*, 134312. (i) Umeda, R.; Hibi, D.; Miki, K.; Tobe, Y. *Pure Appl. Chem.* **2010**, *82*, 871.
- (16) (a) Di Motta, S.; Negri, F.; Fazzi, D.; Castiglioni, C.; Canesi, E. V. *J. Phys. Chem. Lett.* **2010**, *1*, 3334. (b) Fazzi, D.; Canesi, E. V.; Negri, F.; Bertarelli, C.; Castiglioni, C. *ChemPhysChem* **2010**, *11*, 3685.
- (17) (a) Stoll, H.; Savin, A. In *Density Functional Methods in Physics*; Dreizler, R., da Providencia, J., Eds.; Plenum: New York, 1985; p 177. (b) Ikura, H.; Tsuneda, T.; Yanai, T.; Hirao, K. *J. Chem. Phys.* **2001**, *115*, 3540. (c) Tawada, Y.; Tsuneda, T.; Yanagisawa, S.; Yanai, T.; Hirao, K. *J. Chem. Phys.* **2004**, *120*, 8425.
- (18) (a) Herebian, D.; Wiegardt, K. E.; Neese, F. *J. Am. Chem. Soc.* **2003**, *125*, 10997. (b) Kubo, T. *Doctoral Thesis*, Osaka University, Japan, 1996.
- (19) (a) Yamaguchi, K. In *Self-Consistent Field: Theory and Applications*; Carbo, R.; Klobukowski, M., Eds.; Elsevier: Amsterdam, 1990; p 727. (b) Hayes, E. F.; Siu, A. K. Q. *J. Am. Chem. Soc.* **1971**, *93*, 2090. (c) Takatsuka, K.; Fueno, T.; Yamaguchi, K. *Theor. Chim. Acta* **1978**, *48*, 175. (d) Head-Gordon, M. *Chem. Phys. Lett.* **2003**, *372*, 508. (e) Yamaguchi, K. In *Organometallic Conjugation*; Nakamura, A.; Ueyama, N.; Yamaguchi, K., Eds.; Kodansha and Springer: Tokyo, 2002; p 29. (f) Nakano, M.; Fukui, H.; Minami, T.; Yoneda, K.; Shigeta, Y.; Kishi, R.; Champagne, B.; Botek, E.; Kubo, T.; Ohta, K.; Kamada, K. *Theor. Chem. Acc.* **2011**, DOI 10.1007/s00214-010-0871-y.
- (20) Cohen, H. D.; Rootaan, C. C. J. *J. Chem. Phys.* **1965**, *43*, S34.
- (21) (a) Hurst, G. J. B.; Dupuis, M.; Clementi, E. *J. Chem. Phys.* **1988**, *89*, 385.
- (22) (a) Sekino, H.; Bartlett, R. J. *J. Chem. Phys.* **1993**, *98*, 3022. (b) Yamada, S.; Nakano, M.; Shigemoto, I.; Kiribayashi, S.; Yamaguchi, K. *Chem. Phys. Lett.* **1997**, *267*, 445. (c) Maroulis, G. *J. Chem. Phys.* **1998**, *108*, 5432. (d) Kamada, K.; Ueda, M.; Nagao, H.; Tawa, K.; Sugino, T.; Shimizu, Y.; K. Ohta, K. *J. Phys. Chem. A* **2000**, *104*, 4723. (e) Champagne, B.; Botek, E.; Nakano, M.; Nitta, T.; Yamaguchi, K. *J. Chem. Phys.* **2005**, *122*, 114315. (f) O'Neill, D. P.; Kallay, M.; Gauss, J. J.

*Chem. Phys.* **2007**, *127*, 134109. (g) Maroulis, G. *J. Chem. Phys.* **2008**, *129*, 044314. (h) Hammond, J. R.; Kowalski, K. *J. Chem. Phys.* **2009**, *130*, 194108. (i) Baranovska, A.; Sadlej, A. J. *J. Comput. Chem.* **2010**, *31*, 552. (j) de Wergifosse, M.; Champagne, B. *J. Chem. Phys.* **2011**, *134*, 074113.

(23) Nakano, M.; Kubo, T.; Kamada, K.; Ohta, K.; Kishi, R.; Ohta, S.; Nakagawa, N.; Takahashi, H.; Furukawa, S.; Morita, Y.; Nakasuji, K.; Yamaguchi, K. *Chem. Phys. Lett.* **2006**, *418*, 142.

(24) (a) Nakano, M.; Shigemoto, I.; Yamada, S.; Yamaguchi, K. *J. Chem. Phys.* **1995**, *103*, 4175. (b) Nakano, M.; Yamaguchi, K. *Chem. Phys. Lett.* **1993**, *206*, 285. (c) Nakano, M.; Yamada, S.; Shigemoto, I.; Yamaguchi, K. *Chem. Phys. Lett.* **1996**, *251*, 381.

(25) Frisch, M. J.; Trucks, G. W.; Schlegel, H. B.; Scuseria, G. E.; Robb, M. A.; Cheeseman, J. R.; Scalmani, G.; Barone, V.; Mennucci, B.; Petersson, G. A.; et al. *Gaussian 09*, Revision A.1; Gaussian, Inc: Wallingford, CT, 2009.

(26) Ovchinnikov, A. A. *Theor. Chim. Acta* **1978**, *47*, 297.